Optimal design and operation of large-scale heat pumps in district heating and cooling systems

Marco Wirtz[a](CA), Lukas Kivilip[a], Peter Remmen[a] and Dirk Müller[a]

[a] *RWTH Aachen University, E.ON Energy Research Center, Institute for Energy Efficient Buildings and Indoor Climate, Aachen, Germany, marco.wirtz@eonerc.rwth-aachen.de*

Abstract:

The integration of power-to-heat technologies, especially heat pumps, into district heating systems is a promising approach to increase the efficiency of local energy systems and simultaneously offer flexibility to the electric power grid. If a cooling network exists alongside the heating network, the return line of the cooling network can serve as heat source for a large-scale central heat pump. In this system setup, a heat pump couples the heating and cooling networks with each other. This enables cooling down the return line of the cooling network and simultaneously pre-heating the return line of the heating network. The design of these integrated systems is challenging and is increasingly carried out with mathematical optimization methods. In this work, we present a mixed-integer linear program (MILP) for designing district heating and cooling systems coupled with a large-scale heat pump. The result is an optimized design and operation of the heat pump integrated in the overall energy supply system, which includes also conventional technologies such as gas boilers, combined heat and power units, compression and absorption chillers. The MILP model is applied to a district heating and cooling system of a research campus in Germany. The installation of a central heat pump leads to cost savings of 6 % and a CO_2 reduction of 38 % compared to a benchmark design without heat pump. If lower temperatures in the heating network can be realized, the heat pump operates at higher COPs and meets larger shares of the network demands, which leads to further cost savings of 12 %.

Keywords:

District heating, District cooling, Heat pump, Mixed-integer linear programming, Multi-objective optimization.

1. Introduction

The heating and cooling sector is estimated to use half of the total energy consumed in Europe [1]. District heating and cooling systems are one solution to reduce the energy consumption and, thus, reduce the CO_2 emissions. Modern, so-called 4th generation, district heating systems operate at temperatures below 70 °C. Low network temperatures favor the integration of efficient large-scale heat pumps with small temperature lifts [2].

The integration of large-scale heat pumps into district heating systems has already been widely investigated in literature: Averfalk et al. [3] provide an overview about large-scale heat pumps in district heating systems in Sweden and stress the flexibility provided by power-to-heat installations. Blarke et al. [4] analyze the consequences of integrating large-scale heat pumps into the district

heating systems: On the one hand, heat pumps increase the flexibility of the system to buffer peaks in renewable electricity production. On the other hand, the integration of heat pumps into supply systems with CHPs reduce the operation hours of CHP engines. In order to enhance the integration of renewables in the energy system, Lund et al. [5] suggest to integrate heat pumps into CHP supply stations. Molyneaux et al. [6] present a simulation-based optimization of a central plant with a large-scale heat pump, that supplies a district heating network. Lake water serves as heat source for the heat pump. It is shown that heat pumps offer a significant potential for greenhouse gas reduction. Within a simulation study, Østergaard et al. [7] investigate the integration of small booster heat pumps in buildings together with large-scale heat pumps at central supply stations. The lower network temperatures result in lower thermal losses and a higher efficiency of the central heat pump.

There are numerous different heat sources used by large-scale heat pumps: Sewage water, ambient water, industrial waste heat, geothermal water, flue gas and district cooling. Especially the integration into district cooling systems is a promising approach since both heat flows of the heat pump are used to serve the system: The evaporator produces cold, the condenser heat. In Scandinavia, large-scale heat pumps are in operation that use the return pipe of district cooling as heat source [8]. Especially in industry and commercial districts in Scandinavia, this supply concept is of growing interest.

Designing energy supply systems that cover heating and cooling demands with various energy resources in a reliable, economic and environmental-friendly manner is a complex task and calls for optimization analysis [9]. In this field, mathematical programming is one important tool. In the following, we present scientific works which utilize mathematical programming and include heat pumps in their system structure: Pavičević et al. [10] present a mixed-integer linear program (MILP) for designing an optimal supply system for a district heating networks. The superstructure includes large-scale air-source heat pumps. The COP of the heat pump is calculated based on the ambient air temperature and varies between 2 and 3.5. Bohlayer et al. [11] present a MILP formulation for the integration of low temperature waste heat into an energy supply system of a manufacturing company. Here, different temperature levels of waste heat sources are considered and heat pumps for different temperature lifts are designed.

We present a MILP formulation for the optimal integration of large-scale heat pumps into heating and cooling networks. The superstructure of the model incorporates gas boiler, CHP, compression and absorption chiller as well as a large-scale heat pump. The methodology is applied to a real-world example. Based on the use case, we analyze to which extend heat pumps can contribute to the supply of heat and cold, and how the integration affects the optimal capacities of other technologies in a trigeneration system. The work is structured as follows: In section 2, we present the MILP model together with the underlying superstructure. In section 3, the use case and three different scenarios are introduced. The results are presented for all scenarios in section 4. The paper concludes with a discussion of the findings in section 5.

2. Methodology

In this section, we describe the optimization model and the underlying assumptions. In section 2.1, we present the superstructure of the model. The superstructure contains the entire set of technologies from which the optimal configuration is chosen within the optimization process. In section 2.2, the MILP formulation is presented.

2.1. System superstructure

The investigated energy supply system is a conventional district heating and cooling network. The distribution networks are modeled without considering dynamic effects. Thermal network losses are calculated in a pre-processing step. The heating and cooling demands of all buildings are aggregated with the thermal network losses to one heat and cold demand time series for one year with an hourly time resolution. The thermal networks are supplied by a central energy hub. The superstructure is depicted in Fig. 1. It incorporates a gas boiler, CHP as well as a compression and absorption chiller. The compression chiller is driven by electric power. Heat from the gas boiler or CHP can be utilized

for driving the absorption chiller. A central large-scale heat pump is placed between the heating and cooling network. During operation, the heat pump cools down the cooling network in its evaporator. At the same time, the return line of the heating network serves as the heat pump's heat sink. The heat pump serves therefore as a heating and cooling supply unit at the same time. The temperature lift of the heat pump depends on the network temperatures. The evaporation temperature of the heat pump must be lower than the return temperature of the cooling network ($T_{c,return}$), and the condenser temperature must exceed the return temperature of the heating network ($T_{h,return}$). As a result, for lower heating network or higher cooling network temperatures, the temperature lift is smaller and higher COPs can be achieved. The electric power consumed by the heat pump is supplied by the electric power grid or by the CHP.
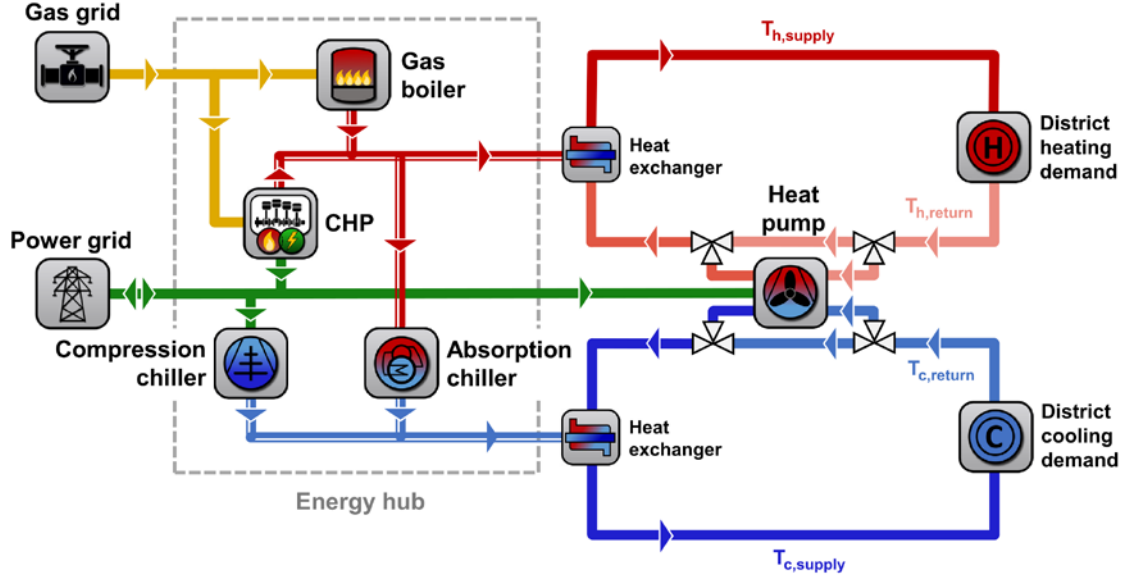

Figure 1. Schematic overview of optimization superstructure with integrated heat pump between the cooling and heating network.

2.2. MILP formulation

In the following, the objective functions and constraints of the MILP formulation are described in detail. The proposed model optimizes the structure, sizing and operation of all energy conversion technologies. Decision variables in the model are highlighted in bold. All variables are constrained to have non-negative values unless otherwise stated. In the formulation, $\dot{Q}_h$ and $\dot{Q}_c$ denote heat and cold flows, respectively.

2.2.1. Objective functions

In this work, a multi-objective approach is chosen: Pareto-optimal solutions are calculated based on the ε-constraint method. As objective functions, we consider total annualized costs (TAC) as well as CO_2 emissions. The calculation of the TAC is based on the German guideline VDI 2067 [12] and includes investment costs $C^{inv,tot}$, operation and maintenance costs $C^{o\&m}$ as well as electricity C^{el} and gas costs C^{gas}. In this formulation, electricity costs include the revenues from electricity feed-in. Thus, the TAC (C^{TAC}) are defined as

$$\min C^{TAC} = C^{inv,tot} + C^{o\&m} + C^{el} + C^{gas} \tag{1}$$

Here, the investment costs of all components k (together with constant investment costs for the thermal network) add up to the total investment costs $C^{inv,tot}$

$$C^{inv,tot} = \sum_k C^{inv}_k + C^{inv}_{netw} \tag{2}$$

In practice, the relationship between the component's capacity and investment cost is non-linear. Therefore, as suggested in [13], we express this non-linearity with a piece-wise linear approximation based on manufacturer and literature data. For this purpose, we introduce auxiliary variables $\xi_{k,i}$ for each component k and a number of supporting points N_k^ξ. These additional variables couple the investment costs with the rated power of the component. The investment cost for component k is expressed by

$$C_k^{\text{inv}} = \sum_{i=1}^{N_k^\xi} \xi_{k,i} I_{k,i} \tag{3}$$

in which N_k^ξ is the number of supporting points and $I_{k,i}$ the investment costs at supporting point i. Thus, the rated heating ($\overline{Q}_h$), cooling ($\overline{Q}_c$) or electric ($\overline{P}_{el}$) power of the respective components are

$$\overline{Q}_{h,k} = \sum_{i=1}^{N_k^\xi} \xi_{k,i} cap_{k,i} \quad \forall\, k \in \{BOI, HP\} \tag{4a}$$

$$\overline{P}_{el,CHP} = \sum_{i=1}^{N_k^\xi} \xi_{CHP,i} cap_{CHP,i} \tag{4b}$$

$$\overline{Q}_{c,k} = \sum_{i=1}^{N_k^\xi} \xi_{k,i} cap_{k,i} \quad \forall\, k \in \{CC, AC\} \tag{4c}$$

with $cap_{k,i}$ as the rated capacity at supporting point i. In addition, the sum of all auxiliary variables must equal 1:

$$\sum_{i=1}^{N_k^\xi} \xi_{k,i} = 1 \tag{5}$$

Furthermore, for each component a Special Ordered Set 2 (SOS2) is introduced that implies that at most two neighboring entries within $\xi_{k,i}$ for component k can be greater than zero [14]. The solver used in this study supports SOS2; however, the SOS2 relationship can easily be reformulated by introducing additional binary variables [14].

Operation and maintenance costs are modeled as share of the investment costs for all components k:

$$C^{\text{o\&m}} = \sum_k f_k^{\text{o\&m}} C_k^{\text{inv}} \tag{6}$$

In practice, line limits restrict the maximum power that can be withdrawn from the public grid. Larger line limits result in extra costs. Therefore, electricity costs depend on the absolute amount of electrical energy withdrawn from the power grid (working price, EUR / kWh) and on the peak power demand (performance price, EUR / kW). In this model, the peak power demand $\overline{P}_{el,grid}$ is a decision variable and chosen within the optimization. The line limit must be greater or equal to the power withdrawn from or fed into the public distribution grid for all time steps:

$$\overline{P}_{el,grid} \geq P_{el,grid,t} \quad \forall\, t \tag{7a}$$

$$\overline{P}_{el,grid} \geq P_{el,feed-in,t} \quad \forall\, t \tag{7b}$$

Thus, the electricity costs sum up to

$$C_{el} = \overline{P}_{el,grid}\, p_{el,peak} + \sum_t P_{el,grid,t}\, p_{el,work} - \sum_t P_{el,feed-in,t}\, p_{el,feed-in} \tag{8}$$

All cost parameters are listed in Table 1. Likewise, gas costs are modeled with a working and a performance price. The maximum gas withdrawal $\overline{G_{grid}}$ from the gas grid depends on the gas demand of the CHP $\dot{G}_{CHP,t}$ and boiler $\dot{G}_{BOI,t}$, which is expressed by

$$\overline{G_{grid}} \geq \dot{G}_{BOI,t} + \dot{G}_{CHP,t} \quad \forall\, t \tag{9}$$

The total gas costs sum up to

$$C^{gas} = \overline{G_{grid}}\, p_{gas,peak} + \left(\sum_t \dot{G}_{BOI,t} + \sum_t \dot{G}_{CHP,t} \right) p_{gas,work} \tag{10}$$

The second objective function are the total annual CO_2 emissions e^{tot}. Carbon emissions are caused by the combustion process in the gas-fired components (here CHP and boiler) and the electricity imports from the public distribution grid. Therefore, the total CO_2 emissions are

$$e^{tot} = e^{gas} \left(\sum_t \dot{G}_{BOI,t} + \sum_t \dot{G}_{CHP,t} \right) + e^{el,grid} \sum_t P_{el,grid,t} \tag{11}$$

Table 1. Energy costs and specific CO2 emissions

Parameter	Symbol	Unit	Value
Performance price for electricity	$p_{el,peak}$	EUR / kW	59.66
Working price for electricity	$p_{el,work}$	EUR / kWh	0.145
Revenue for electricity feed-in	$p_{el,feed-in}$	EUR / kWh	0.064
Performance price for natural gas	$p_{gas,peak}$	EUR / kW	12.15
Working price for natural gas	$p_{gas,work}$	EUR / kWh	0.028
Specific CO2 emissions natural gas	e^{gas}	kg / kWh	0.200
Specific CO2 emissions electricity import	$e^{el,grid}$	kg / kWh	0.503

2.4.2. Model constraints

In this section, the constraints for each technology are presented. The efficiencies of all components are assumed constant and no part-load specific behavior is considered. Thus, for the boiler (BOI) and CHP the governing equations are

$$\dot{Q}_{h,BOI,t} = \eta_{th,BOI}\, \dot{G}_{BOI,t} \quad \forall\, t \tag{12a}$$

$$\dot{Q}_{h,CHP,t} = \eta_{th,CHP}\, \dot{G}_{CHP,t} \quad \forall\, t \tag{12b}$$

$$P_{el,CHP,t} = \eta_{el,CHP}\, \dot{G}_{CHP,t} \quad \forall\, t \tag{12c}$$

Here, $\dot{Q}_{h,BOI,t}$ and $\dot{Q}_{h,CHP,t}$ denotes the heat output of the boiler and CHP respectively. $\dot{G}_t$ is the gas demand on each time step. The thermal efficiency of the boiler and CHP is 0.9 and 0.45, respectively. The electric efficiency of the CHP is 0.42. The thermal power of the gas boiler and the electric power of the CHP is limited by their rated power ($\overline{Q}_{h,BOI}/\overline{P}_{el,CHP}$):

$$\dot{Q}_{h,BOI,t} \leq \overline{Q}_{h,BOI} \quad \forall\, t \tag{13a}$$

$$P_{el,CHP,t} \leq \overline{P}_{el,CHP} \quad \forall\, t \tag{13b}$$

Cooling power can be provided by compression chiller (CC) and absorption chiller (AC). The cooling power provided by the chillers is given by

$$\dot{Q}_{c,CC,t} = COP_{CC}\, P_{el,CC,t} \quad \forall\, t \tag{14a}$$

$$\dot{Q}_{c,AC,t} = COP_{AC}\, \dot{Q}_{h,AC,t} \quad \forall\, t \tag{14b}$$

Here, $P_{el,CC,t}/\dot{Q}_{h,AC,t}$ represents the electric and thermal power demand of the compression and absorption chiller. COP_{AC} denotes the ratio of provided cooling power and consumed heat and is 0.68. The cooling output of the chillers is limited by their rated cooling power:

$$\dot{Q}_{c,k,t} \leq \overline{\dot{Q}}_{c,k} \quad \forall \, k \in \{CC, AC\} \; \forall \, t \tag{15}$$

The coefficient of performance COP_{HP} couples the electricity demand of the large-scale heat pump $P_{el,HP,t}$ with its heating power $\dot{Q}_{h,HP,t}$:

$$\dot{Q}_{h,HP,t} = COP_{HP} \; P_{el,HP,t} \quad \forall \, t \tag{16}$$

An energy balance around the heat pump provides the heat flow to the evaporator:

$$\dot{Q}_{c,HP,t} = \dot{Q}_{h,HP,t} - P_{el,HP,t} \quad \forall \, t \tag{17}$$

The heat provided by the heat pump (at the condenser) is limited by the rated thermal power:

$$\dot{Q}_{h,HP,t} \leq \overline{\dot{Q}}_{h,HP} \quad \forall \, t \tag{18}$$

The COP of heat pumps strongly depends on the evaporator and condenser temperatures. By lowering the temperature lift between heat source and sink, the COP is increased significantly. In this study, the heat pump is mass-flow controlled, which enables a stationary mode of operation with respect to the temperature levels, and thus the evaporator and condenser temperature are assumed constant over time. The heat pump's COP is calculated based on a model presented by [15], which gives a thermodynamic-based estimation for large-scale ammonia heat pumps. The COP of the compression chiller is modeled accordingly, deriving the condenser temperature from the ambient air temperature. In order to avoid unrealistic large COPs, which can occur for very low temperature lifts, the heat pump's COP is limited to 7 and the chiller's COP to 6.

2.4.3. Energy balances

The heating and cooling power of all technologies have to be in balance with the thermal demands of the heating and cooling networks. This is expressed by three energy balances, as described in the following: For the heat balance the governing equation is

$$\dot{Q}_{h,BOI,t} + \dot{Q}_{h,CHP,t} + \dot{Q}_{h,HP,t} = \dot{Q}_{h,dem,t} + \dot{Q}_{h,loss,t} + \dot{Q}_{h,AC,t} \quad \forall \, t \tag{19}$$

Here, $\dot{Q}_{h,dem,t}$ describes the heating demand of all buildings connected to the heating network and $\dot{Q}_{h,loss,t}$ represents thermal network losses to the ground. In order to estimate thermal losses, the soil temperature is modeled as proposed in [16]. Due to the high temperature level needed by the absorption chiller, the following constraint ensures that the heat driving the absorption chiller can only be supplied by the boiler and/or CHP, but not from the heat pump:

$$\dot{Q}_{h,BOI,t} + \dot{Q}_{h,CHP,t} \geq \dot{Q}_{h,AC,t} \quad \forall \, t \tag{20}$$

The thermal demand of the cooling network (including thermal losses) has to equal the cooling power provided by the heat pump, compression and absorption chiller:

$$\dot{Q}_{c,CC,t} + \dot{Q}_{c,AC,t} + \dot{Q}_{c,HP,t} = \dot{Q}_{c,dem,t} + \dot{Q}_{c,loss,t} \quad \forall \, t \tag{21}$$

Electric power from the CHP can be used by the heat pump and compression chiller. In addition, electricity can be withdrawn from or fed into the public electricity grid ($P_{el,grid,t}$, $P_{el,feed-in,t}$). Electrical losses in the power grid as well as pump work in the thermal network are neglected since the pump work usually accounts for less than 1 % of the heat delivery [17]. Thus, the power balance is:

$$P_{el,CHP,t} + P_{el,grid,t} = P_{el,feed-in,t} + P_{el,HP,t} + P_{el,CC,t} \quad \forall \, t \tag{22}$$

Due to technical limitations, commercial heat pumps cannot generate temperatures above 90 °C [18]. If the supply network temperature ($T_{h,supply}$) exceeds this temperature, the boiler or the CHP engine has to run in order to rise the temperature to the needed temperature level. Therefore, the share of the heat demand that can be covered by the heat pump for a certain time step is limited by

$$\dot{Q}_{h,HP,t} \leq \frac{\Delta T_{cond}}{T_{h,supply} - T_{h,return}} \; \dot{Q}_{h,dem,t} \quad \forall \, t \tag{23}$$

Here, ΔT_{cond} describes the temperature rise in the condenser of the heat pump and $T_{\text{h,return}}$ denotes the return temperature of the heating network. Likewise, the thermal power of the evaporator (cooling power of heat pump) is limited by

$$\dot{Q}_{\text{c,HP},t} \leq \frac{\Delta T_{\text{evap}}}{T_{\text{c,return}} - T_{\text{c,supply}}} \, \dot{Q}_{\text{c,dem},t} \quad \forall\, t \tag{24}$$

Here, ΔT_{evap} describes the temperature decrease in the evaporator of the heat pump across the return line of the cooling network. $T_{\text{c,return}}$ and $T_{\text{c,supply}}$ denote the supply and return temperature of the cooling network, respectively.

3. Case study and supply scenarios

3.1. Use case

We apply the proposed methodology to a model district with 17 buildings. As input data, we use measured heating and cooling demands of buildings on a research campus in Germany (FZ Jülich). The data stock comprises predominantly office buildings as well as a data center. The daily mean of the total heating and cooling demand of the buildings is depicted for one year in Fig. 2. A large share of the cooling demand results from the data center. The annual heating demand is 6.36 GWh, the annual cooling demand 10.04 GWh. The hourly peak heat demand is 2.01 MW, the peak cold demand is 2.42 MW. In order to investigate the heat pump integration for different network temperatures, three scenarios are investigated: Scenario 1 and 2 are based on measured network temperatures. In Scenario 3, the temperature of the heating network is assumed lower, similar to modern low temperature networks.
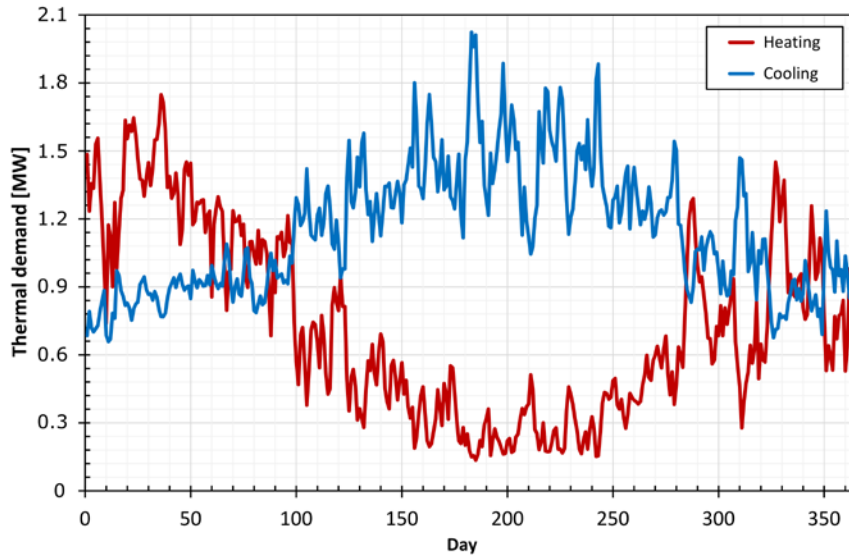

Figure 2. Cumulated daily mean of the building's heating and cooling demands.

3.2. Scenario 1: Base case without heat pump

For comparison purposes, as a first scenario, the optimal energy supply system without heat pump is investigated. Therefore the additional constraint

$$\overline{Q_{\text{h,HP}}} = 0 \tag{25}$$

is introduced in this scenario. All heating and cooling demands are covered by the gas boiler, CHP, compression or absorption chiller.

3.3. Scenario 2: High temperature network with central heat pump

In this scenario, the heat pump can be installed within the optimization. Like in Scenario 1, the supply temperature of the district heating network is controlled within a temperature interval of

$T_{h,supply}$ = 95–140 °C (depending on the ambient air temperature). The return temperature is constant $T_{h,return}$ = 70 °C. The supply temperature of the cooling network is $T_{c,supply}$ = 6 °C, and the return temperature $T_{c,return}$ = 12 °C.

3.4. Scenario 3: Low temperature network with central heat pump

Scenario 3 differs from Scenario 2 only in terms of supply and return temperatures of the heating network as well as the supply temperature of the heat pump. This network represents a modern low temperature network (4th generation district heating). The supply temperature of the heating network is assumed 60 °C and the return temperature 30 °C. The network temperatures of the cooling network are the same as in Scenario 2.

4. Results

In this section, the optimization results for all scenarios are described. At first, we analyze the optimal supply temperature of the heat pump for Scenario 2 and 3. Then, we present the optimal energy systems in more detail.

4.1. Optimal condenser temperature

One key parameter of the model is the supply temperature of the heat pump, which describes the outlet temperature of the condenser. This temperature affects the temperature rise across the condenser of the heat pump (ΔT_{cond}), and according to (23) the share of the heat demand that can be covered by the heat pump. A high supply temperature allows covering a larger share of the heat demand with the heat pump. However, at high supply temperatures, the COP decreases due to the larger temperature difference between condenser and evaporator. In Scenario 2, the decrease of the COP with higher supply temperature is small and within a range of 0.4 (COP$_{6->70 °C}$ = 3.1, COP$_{6->90 °C}$ = 2.7). However, in Scenario 3, the decrease of the COP with larger temperature lifts becomes more relevant (COP$_{6->30 °C}$ = 7.0, COP$_{6->60 °C}$ = 4.2). Therefore, choosing the optimal supply temperature of the heat pump is not trivial. In order to determine the optimal condenser temperature, a parameter study is conducted.

For Scenario 3, the total annualized costs for different supply temperatures in the interval between 30 °C and 60 °C are depicted in Fig. 3. Supply temperatures below 30 °C are not possible, since this is lower than the return temperature of the heating network. Likewise, supply temperatures above 60 °C are not reasonable, since the supply temperature of the heat pump would exceed the supply temperature of the network, which leads to unnecessary exergy losses. As depicted in Fig. 3, TAC (black line) decrease with increasing supply temperatures of the heat pump until 50 °C. Above 50 °C, the total annualized costs increase again slightly. The optimal energy system with a supply temperature of 50 °C shows a cost reduction of 16 % compared to the optimal system with 30 °C. The TAC of supply temperatures above 50 °C are within a range of 2 %.

For Scenario 2, the optimal supply temperature is 90 °C. Here, a larger contribution of the heat pump to the heat production is preferred over a slightly higher COP. Thus, the heat pump can pre-heat the return line of the heating network from 70 °C to 90 ° C (ΔT_{cond} = 20 °C). The heat pump therefore realizes a temperature lift from 6 °C to 90° C (excluding the temperature drop across the internal heat exchangers). Since the supply temperature of the heating network exceeds 90 °C throughout the year, the heat pump cannot cover the heat demand in any point of time completely. According to (23) the maximum share of the heat demand that can be covered by the heat pump in each time step varies between 0.8 in summer ($T_{h,supply}$ = 95 °C) and 0.29 in winter ($T_{h,supply}$ = 140 °C). According to (24), the maximum share of the cooling demand that can be provided by the heat pump is 1 all year round.
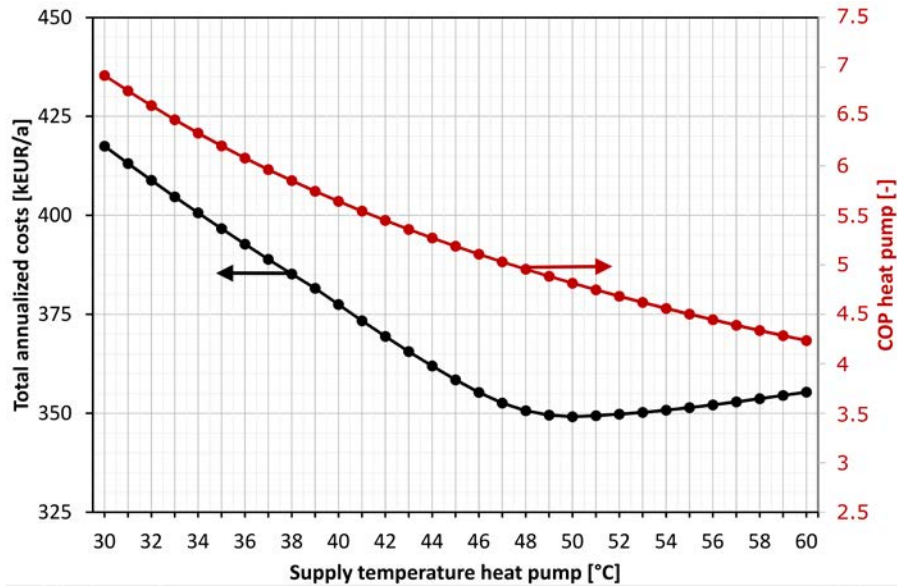
Figure 3. TACs and COPs for different supply temperatures of the heat pump in Scenario 3.

4.2. Optimal energy supply system

In the following, we present the optimal energy supply systems (with optimal supply temperatures of the heat pump as described in the previous section). Table 2 provides an overview of the numerical results for the cost-optimal anchor point for each scenario. The cost optimal anchor point refers to a solution from the set of cost optimal solutions that has the least CO_2 emissions.

Table 2. Result overview for cost optimal solution.

Performance indicator	Unit	Scenario 1	Scenario 2	Scenario 3
Total annualized costs	kEUR / a	421.2	396.3	349.2
Ann. investment and O&M costs	kEUR / a	183.5	178.0	176.9
Natural gas performance costs	kEUR / a	33.4	21.6	15.6
Natural gas costs	kEUR / a	547.7	339.8	261.0
Electricity performance costs	kEUR / a	43.3	18.1	13.6
Electricity work costs	kEUR / a	0	0.4	1.4
Feed-in revenue	kEUR / a	386.8	161.5	119.2
CO_2 emissions	t / a	3879	2408	1853
COP_{HP}	–	–	2.73	4.82

The lowest TAC (349.2 kEUR / a) are achieved in the low-temperature scenario with heat pump (Scenario 3). This system has 17 % lower costs than the optimal system in Scenario 1 and 12 % lower costs than Scenario 2. This is mainly caused by a significant reduction of gas demand in the two heat pump scenarios. In all scenarios, the gas costs represent a large share of the TAC. This is due to the high CHP load in all scenarios. The CHP supplies electricity to the compression chiller and the heat pump. Excess power is fed into the power grid. Due to lower capacities of the CHP and boiler, the gas costs in Scenario 3 decrease by more than half. In all cases, almost no electricity is drawn from the power grid. The capacity of the power grid connection varies between 0.23 MW (Scenario 3) and 0.73 MW (Scenario 1) is mainly installed in order to feed-in surplus power from the CHP. The resulting electricity performance costs equal about one tenth of the feed-in revenue.

Due to the reduced gas demand, Scenario 3 has the lowest CO_2 emissions. A reduction of 52 % compared to Scenario 1 and 23 % compared to Scenario 2 are observed. The COP of the heat pump is 2.73 in Scenario 2 and 4.82 in Scenario 3. If we consider both thermal flows (heating and cooling) as useful energy flows, the combined COP is 4.46 in Scenario 2 and 8.63 in Scenario 3. The performance improvement of Scenario 3 compared to Scenario 2 is mainly caused by the enhanced

operation of the heat pump, which benefits from an increased COP. The more the heat pump contributes the heat production, the less heat needs to be produced by the CHP, which lowers the gas demand (and at the same time the amount of feed-in power). The main cost reductions are due to reduced fuel costs, whereas investment costs are within a range of 4 % across all scenarios.

In Fig. 4, a) the installed capacities and b) the produced energy of all system components are depicted. The cumulated rated power is similar for all scenarios (approx. 5 MW). However, a decrease of the boiler and CHP capacity is observed from Scenario 1 to 3. As the heat pump supports the heat production in Scenario 2 and 3, the boiler and CHP can be sized smaller. The cooling capacity of the compression and absorption chiller differ only slightly across the scenarios. In Scenario 2 and 3, a heat pump with a heating capacity of 0.66 MW and 1.00 MW respectively is installed. The energy production of the boiler, CHP as well as of the compression chiller reduces from Scenario 1 to 3: The electricity produced by the CHP is 7579 MWh in Scenario 1, and decreases to 3811 MWh in Scenario 3. The boiler meets peak heat demands during winter days in all three scenarios and shows small full load hours (less than 800 h/a in all scenarios).

In order to understand the operation of the system in more detail, in Fig. 5 all a) heat and b) cold flows to and from each component are depicted (monthly averaged). In Fig. 5 a) the produced heat by boiler, CHP and heat pump is illustrated as stacked areas. The heat demands are illustrated as stacked lines (buildings: black, heat demand of the AC: light blue). For a valid energy balance, the top line (demand) and the upper edge of the top area (supply) lie on top of each other. In Fig. 5 b) the cooling balance is depicted in the same manner. Heat pump, compression and absorption chiller generate cold, the only cooling demand is the district cooling network.
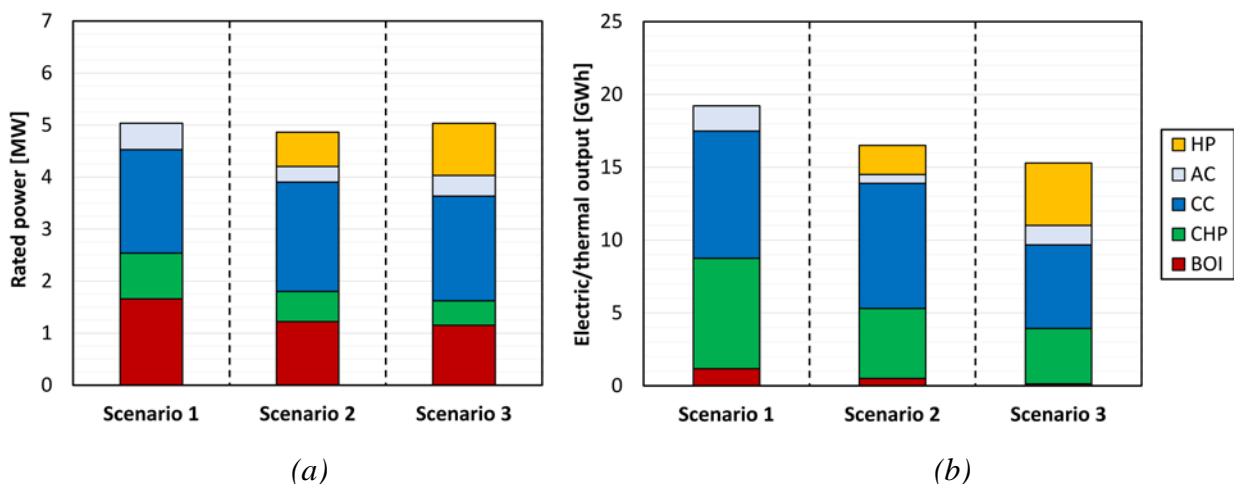

(a)   *(b)*

Figure 4: a) Installed capacity and b) power output of components.

In Scenario 1, the heat is predominantly covered by the CHP. The system is a typical trigeneration system (CCHP). In winter, the excess electricity is used to run the compression chiller. In summer, the boiler is shut down and excess heat from the CHP drives the absorption chiller.

In Scenario 2, the heat pump runs in winter and covers a significant proportion of the heating and cooling demand. In summer, the heat pump is shut down and the cooling demand is covered by compression and absorption chiller. The heat pump is operated with 3032 full load hours.

In Scenario 3, the heat pump reaches the most full load hours (4275 h/a). In this scenario, the boiler is only operated during peak times in winter, resulting in very low full load hours (114 h/a). The CHP has a lower capacity (0.47 MW), and is operated with a high load (8102 full load hours). In this scenario, the heat pump also runs in summer and supports the heat generation of the CHP and the cold generation of the chillers.

Overall, in Scenario 2 and 3, the operation of the heat pump reduces the TAC and CO_2 emissions significantly. The optimal capacities and the operation hours of the CHP decrease. However, this does

not increase the power supply from the power grid but reduces the power feed-in. On the cooling side, the heat pump takes over a significant part of the cooling supply from the chillers.
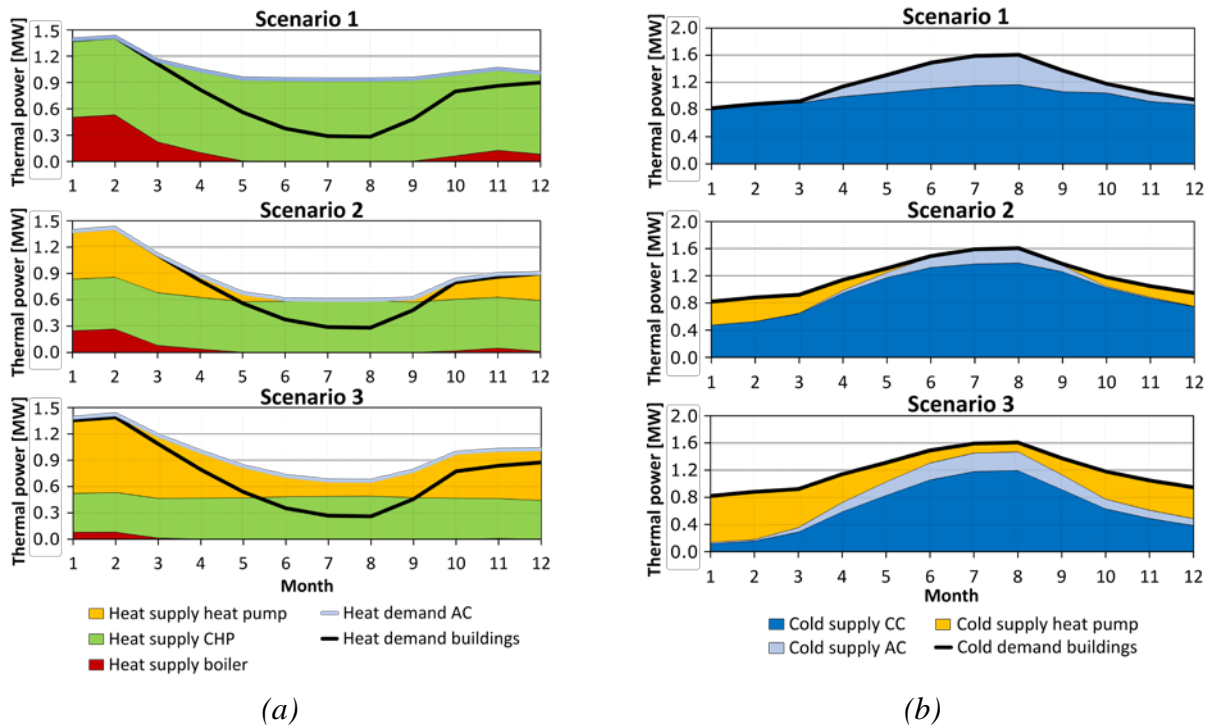

(a)

(b)

Figure 5: a) Heat and b) cold balance for all components and monthly averaged values.

5. Conclusions and outlook

In this work, the optimal integration of large-scale heat pumps into district heating and cooling networks is investigated. For sizing and operation of the energy system a MILP model is developed. The integration of the heat pump between the heating and cooling networks reduces the TAC and CO_2 emissions significantly. In comparison to a base case without heat pump, the CHP and boiler capacities are reduced as well and the gas demand decreases by 38 %. In winter, when heating and cooling demands are about the same size, the heat pump contributes the most to heat and cold generation. Nevertheless, the study shows that even for an optimal operation, the heat pump cannot replace the CHP or boiler completely: The CHP is needed to power the heat pump at low costs. The boiler is needed for peak heat demands, which cannot be met by the CHP or heat pump.

One important design decision is the temperature lift of the heat pump. The smaller the temperature lift, the larger the COP. However, a large temperature lift increases the proportion of the heating and cooling demand that can be met by the heat pump. As shown in this study, the highest temperature lift is not necessarily the most economical solution.

In general, lowering temperatures of the heating network favors the integration of a heat pump into the overall system, mainly due to larger COPs that can be realized. Nevertheless, also for high temperature district heating systems, the integration of a large-scale heat pump can be economic.

In this study, one use case with fixed thermal demands has been investigated. In addition to the network temperature, the demand structure has a significant influence on the efficiency: The integration of the heat pump is more profitable if heating and cooling demands occur simultaneously throughout the year. In future works, one important question that needs to be addressed is how the demand structure affects the optimal design and the economic and ecological potential.

Furthermore, since no dynamic effects or operation details are taken into account in this MILP formulation, the optimal design needs to be verified with the help of detailed simulation models. This way, basic assumptions of the optimization model, like perfect foresight and optimal control, do not

have to be made. Especially, the system control will lower the efficiency and overall performance in practice.

Acknowledgments

References

[1]   European Comission. An EU Strategy on Heating and Cooling, COM(2016) 51 Final 2016.

[2]   Lund H, Østergaard PA, Chang M, Werner S, Svendsen S, Sorknæs P, et al. The status of 4th generation district heating: Research and results. Energy 2018;164:147–59.

[3]   Averfalk H, Ingvarsson P, Persson U, Gong M, Werner S. Large heat pumps in Swedish district heating systems. Renewable and Sustainable Energy Reviews 2017;79:1275–84.

[4]   Blarke M, Lund H. Large-scale heat pumps in sustainable energy systems: System and project perspectives. Therm. sci. 2007;11:143–52.

[5]   Lund H, Werner S, Wiltshire R, Svendsen S, Thorsen JE, Hvelplund F, et al. 4th Generation District Heating (4GDH). Energy 2014;68:1–11.

[6]   Molyneaux A, Leyland G, Favrat D. Environomic multi-objective optimisation of a district heating network considering centralized and decentralized heat pumps. Energy 2010;35:751–58.

[7]   Østergaard PA, Andersen AN. Booster heat pumps and central heat pumps in district heating. Applied Energy 2016;184:1374–88.

[8]   David A, Mathiesen BV, Averfalk H, Werner S, Lund H. Heat Roadmap Europe: Large-Scale Electric Heat Pumps in District Heating Systems. Energies 2017;10:578.

[9]   Sameti M, Haghighat F. Optimization approaches in district heating and cooling thermal network. Energy and Buildings 2017;140:121–30.

[10]   Pavičević M, Novosel T, Pukšec T, Duić N. Hourly optimization and sizing of district heating systems considering building refurbishment – Case study for the city of Zagreb. Energy 2017;137:1264–76.

[11]   Bohlayer M, Zöttl G. Low-grade waste heat integration in distributed energy generation systems - An economic optimization approach. Energy 2018;159:327–43.

[12]   VDI. VDI 2067: Wirtschaftlichkeit gebäudetechnischer Anlagen Grundlagen und Kostenberechnung.

[13]   Majewski DE, Wirtz M, Lampe M, Bardow A. Robust multi-objective optimization for sustainable design of distributed energy supply systems. Computers & Chemical Engineering 2017;102:26–39.

[14]   Williams, Paul H. Model Building in Mathematical Programming: JohnWiley& Sons, Inc.; 2013.

[15]   Jensen JK, Ommen TS, Reinholdt L, Markussen WB, Elmegaard B. Heat pump COP, part 2: Generalized COP estimation of heat pump processes. Proceedings of the13th IIR-Gustav Lorentzen Conference on Natural Refrigerants 2018.

[16]   Badache M, Eslami-Nejad P, Ouzzane M, Aidoun Z, Lamarche L. A new modeling approach for improved ground temperature profile determination. Renewable Energy 2016;85:436–44.

[17]   Frederiksen S, Werner S. District heating and cooling. Lund: Studentliteratur; 2013.

[18]   C. Arpagaus, F. Bless, J. Schiffmann, S. Bertsch. Review on High Temperature Heat Pumps: Market Overview and Research Status. Available from: https://www.ntb.ch/fileadmin/NTB_Institute/IES/bilder/Projekte_TES/91__SCCER-EIP/Review_on_High_Temperature_Heat_Pumps_-_Arpagaus.pdf.